MARS ATMOSPHERE

Strong water isotopic anomalies in the martian atmosphere: Probing current and ancient reservoirs

G. L. Villanueva,[1,2]* M. J. Mumma,[1] R. E. Novak,[3] H. U. Käufl,[4] P. Hartogh,[5] T. Encrenaz,[6] A. Tokunaga,[7] A. Khayat,[7] M. D. Smith[1]

We measured maps of atmospheric water (H_2O) and its deuterated form (HDO) across the martian globe, showing strong isotopic anomalies and a significant high deuterium/hydrogen (D/H) enrichment indicative of great water loss. The maps sample the evolution of sublimation from the north polar cap, revealing that the released water has a representative D/H value enriched by a factor of about 7 relative to Earth's ocean [Vienna standard mean ocean water (VSMOW)]. Certain basins and orographic depressions show even higher enrichment, whereas high-altitude regions show much lower values (1 to 3 VSMOW). Our atmospheric maps indicate that water ice in the polar reservoirs is enriched in deuterium to at least 8 VSMOW, which would mean that early Mars (4.5 billion years ago) had a global equivalent water layer at least 137 meters deep.

We report maps of water isotopologues (H_2O and its deuterated form HDO) across the martian globe, which show strong isotopic anomalies that are difficult to reconcile with simple fractionation processes. These maps address fundamental unknowns such as the current representative ratio of D/H in water and how much water was lost over the geological life of the planet. Isotopic ratios are among the most valuable indicators for the loss of volatiles from an atmosphere. Deuterium fractionation also reveals information about the cycle of water on the planet and informs us of its stability on short- and long-term scales. The vapor pressures of HDO and H_2O differ substantially near the freezing point, making the condensation/sublimation cycle of the isotopologues sensitive to local temperatures and saturation levels and to the presence of aerosol condensation nuclei.

Although many maps of H_2O do exist [e.g., (1, 2)], and some of HDO [e.g., (3, 4)], two-dimensional (2D) maps of atmospheric D/H enrichment on Mars do not. Apart from preliminary 2D maps presented at conferences (5), previous mapping attempts to measure D/H provided only 1D maps of HDO and H_2O based on nearly simultaneous measurements at ground-based infrared (IR) observatories [e.g., (6–9)] or 1D HDO maps (ground-based) and quasisimultaneous H_2O measurements taken from Mars orbit by the Planetary Fourier Spectrometer long-wavelength channel (10). Local isotopic ratios such as derived by Curiosity/ Mars Science Laboratory (MSL) (11) are representative of that specific location and time and may not represent the actual D/H of atmospheric water on Mars (see more below), even though reports of hemispherically averaged D/H in water indicated a similar value of 5 to 6 times the D/H of Earth's oceans [Vienna standard mean ocean water (VSMOW)] (12, 13). Importantly, such isolated (in time and in space) measurements of D/H in the atmosphere were typically—but incorrectly—assumed to be representative of the bulk atmosphere. Spatially resolved measurements of D/H at different times of day and seasons are necessary to disentangle local from global phenomena. Such maps reveal the true isotopic ratio of current water reservoirs, with implications for the global loss of water over geologic time, and may also assist in the identification of new sources of water on Mars.

Currently, the martian atmosphere and surface form an arid and highly inhospitable environment (14, 15). The upper layers of soil were heavily eroded by long-term aeolian activity, and soil chemistry was strongly modified through exposure to energetic photons and particles that penetrated owing to inadequate magnetospheric and atmospheric shielding. However, there is ample evidence that ancient Mars was wet and likely hosted habitable conditions (16, 17), particularly during the Noachian age (3.6 to 4.5 billion years ago), probably leading to the formation of rich subsurface aqueous reservoirs. Moreover, the presence of extensive volcanism likely gave rise to widespread hydrothermal activity and to the formation of diverse chemical environments. Measurements of epithermal neutron fluxes obtained by Mars Odyssey (18) suggest the presence of important near-surface hydrogen concentrations on Mars, and the polar layered deposits (PLD) are estimated to contain ~21 m global equivalent layer (GEL) of water (19, 20). The atmosphere acts as a buffer between the exosphere (at the boundary with outer space) and the main reservoirs of H, C, and O (e.g., regolith and polar caps), with atmospheric isotopic/abundance ratios providing key diagnostics for quantifying the exchange among these environments.

The maps reported herein are based on observations of isotopic water made with high-resolution spectrometers [CRIRES (cryogenic infrared echelle spectrograph), NIRSPEC (near-infrared spectrograph), and CSHELL (cryogenic echelle spectrograph)] at powerful ground-based observatories [VLT (Very Large Telescope), Keck, and IRTF (InfraRed Telescope Facility), respectively] [supplementary materials section 1 (SM-1)]. This program is founded on initial observations performed using NASA's Kuiper Airborne Observatory and the Kitt Peak National Observatory in 1989 (13), and later with IRTF (6, 7). Specifically we targeted the ν_1 band of HDO near 2720 cm^{-1} (3.7 µm) and the $2\nu_2$ band of H_2O near 2990 cm^{-1} (3.3 µm) (see Fig. 1). Spectral lines of these bands on Mars are observable through our atmosphere when measured from high-altitude observatories at moderately high Doppler shifts (>11 km s^{-1}), i.e., when Mars's lines are displaced sufficiently far from the cores of their counterpart telluric absorbing lines. Observations of HDO are additionally favored by the large D/H enrichment present in the martian atmosphere and the strong D/H depletion in terrestrial air at the high altitudes of these observatories (9), which leads to high telluric transmittances. We obtained the greatest sensitivities to HDO and H_2O on Mars by performing observations at times of maximum Doppler shifts, typically several months before or after Mars' closest approach to Earth (every ~2 years).

Mapping was achieved by stepping the spectrometer's entrance slit across the planet and sampling the planet's spectrum at intervals along the slit for each step, leading to full 2D (east-west and north-south) coverage across the observable disk (see details in SM-1). The distance between slit positions was set in accord with observational image quality ("seeing"), guiding precision, and slit width. For a typical Mars diameter of 8″, a slit-width of 0.2″ and a "seeing" of 0.6″, a typical map would consist of 11 slit positions stepped across the planet, with a minimum of 9 positions for less favorable conditions. For each slit position, abundance measurements are obtained at intervals of 0.6″ along the slit. The maps are of relatively high spatial resolution (~500 km near sub-Earth positions), and, importantly, each map was obtained within a short time interval (1 to 2 hours), thereby providing hemiglobal snapshots in time that are critical for investigating the effects of local phenomena (e.g., orographic clouds and planet-scale waves) and transient processes (e.g., polar releases and diurnal effects).

The data reported here were collected over several years and seasons on Mars from March 2008 until January 2014. From this database, we made a localized D/H measurement over the Viking 1 landing site (9) and obtained a comprehensive search for organics in the martian atmosphere (15). Here, we present results from the best data sets targeting D/H, obtained at times

[1]NASA Goddard Space Flight Center, Greenbelt, MD 20771, USA. [2]Catholic University of America, Washington, DC 20064, USA. [3]Iona College, New Rochelle, NY 10801, USA. [4]European Southern Observatory, Munich, Germany. [5]Max Planck Institute for Solar System Research, Katlenburg-Lindau 37191, Germany. [6]Observatoire de Paris-Meudon, Meudon 92195, France. [7]University of Hawaii-Manoa, Honolulu, HI 96822, USA.
*Corresponding author. E-mail: geronimo.villanueva@nasa.gov

of low telluric water, high Doppler shift, and maximum spatial coverage (CRIRES, 8–9 September 2009; CSHELL, 25 March 2008; NIRSPEC, 24 January 2014; CRIRES 29–30 January 2014) (see Fig. 2 and fig. S1). The data span seasons from late northern winter to late northern spring on Mars (areocentric longitude or season L_s = 335°, 50°, 80°, and 83°) and sample the critical interval when the northern polar cap sublimates and replenishes the atmosphere with water.

The highest spectral resolution is achieved with the narrow slit (0.2″) of CRIRES, leading to a resolving power of $\lambda/\delta\lambda$ ~100,000, whereas the cross-dispersed feature of NIRSPEC provides the broadest spectral coverage at a high resolving power of $\lambda/\delta\lambda$ ~40,000. Such broad spectral coverage allows us to sample HDO and H_2O with a single NIRSPEC setting, whereas measurements with CRIRES and CSHELL require mappings at two spectral settings (3.7 μm and 3.3 μm). Each setting also samples lines of CO_2 that we use to establish the total atmospheric column and to quantify extinction and scattering effects by water ice and dust aerosols (SM-2). Abundance ratios and column densities for H_2O and HDO at each footprint are then corrected for local (spatial and spectral) variations in the comeasured CO_2 column, removing an important source of systematic error that would otherwise affect isotopic measurements. We derive molecular column densities at each footprint by comparing the residual spectrum to a synthetic Mars spectrum (color traces in Fig. 1), itself affected by the mono-

chromatic telluric transmittance for each spectral line at its Mars Doppler-shifted spectral position. For this process, we employ the efficient and robust Levenberg-Marquardt curve-fitting method, which also provides reliable error estimates as derived from the measured Jacobians (SM-1). We typically obtain high signal-to-noise ratios of ~70 for the HDO columns with CRIRES, but the precision of the D/H ratio is defined mainly by the H_2O columns. The median accuracy of the D/H measurements is 0.2, 0.5, 0.8, and 0.4 VSMOW for the January 2014 CRIRES, January 2014 NIRSPEC, September 2009 CRIRES, and March 2008 CSHELL observations, respectively.

The H_2O and HDO disk maps (Fig. 2) reveal strong local anisotropies and seasonal variability. The slow replenishing of water vapor in the northern hemisphere as the polar cap sublimates during northern spring is quite noticeable, in particular when compared to the baseline measurements in late northern winter (L_s 335°). Variability of H_2O with latitude and season is apparent (Fig. 2) and is generally consistent with previous spacecraft measurements of the water cycle (21, 22). HDO maps superficially resemble those of H_2O in showing strong variability, but their direct comparison reveals strong differences that are most easily seen in the maps of the ratio of D/H enrichment in water vapor, relative to Earth's oceans (VSMOW).

The maps of D/H enrichment show a remarkably different evolution and structure compared with total water, with an apparent relationship

to topography and atmospheric temperature. Low D/H values are seen at high altitudes, whereas high D/H values are seen in basins and orographic depressions. Very low D/H [1 to 3 VSMOW] appears in the winter hemisphere, but the spring hemisphere shows much higher values. The vapor pressure isotope effect, which produces an isotopic fractionation at condensation (e.g., cloud formation and frost/ground fog formation), could explain some of this latitudinal variability, yet the observed localized (in time and space) anisotropies are certainly higher than was predicted by current atmospheric models (23, 24). For instance, preferential condensation of HDO could perhaps explain the strong D/H depletion seen in clouds over Elysium Mons on 24 January 2014 and similarly over the Tharsis district as observed in September 2009 and January 2014. Interestingly, strong clouds are observed over this region by the Mars Color Imager camera onboard the Mars Reconnaissance Orbiter (25). As discussed in (24), Rayleigh distillation would provide the strongest isotopic fractionation, yet (on Mars) competition between condensation and sedimentation may lead to certain nonequilibrium fractions, while kinetic processes may enhance or diminish the efficiency of fractionations on Mars as is observed on Earth (26).

Importantly, our maps reveal notably higher deuterium enrichment than was found in globally averaged observations that indicated D/H values of 5.0 ± 0.2 VSMOW (13) and 5.8 ± 2.6 VSMOW (12). This difference is expected because
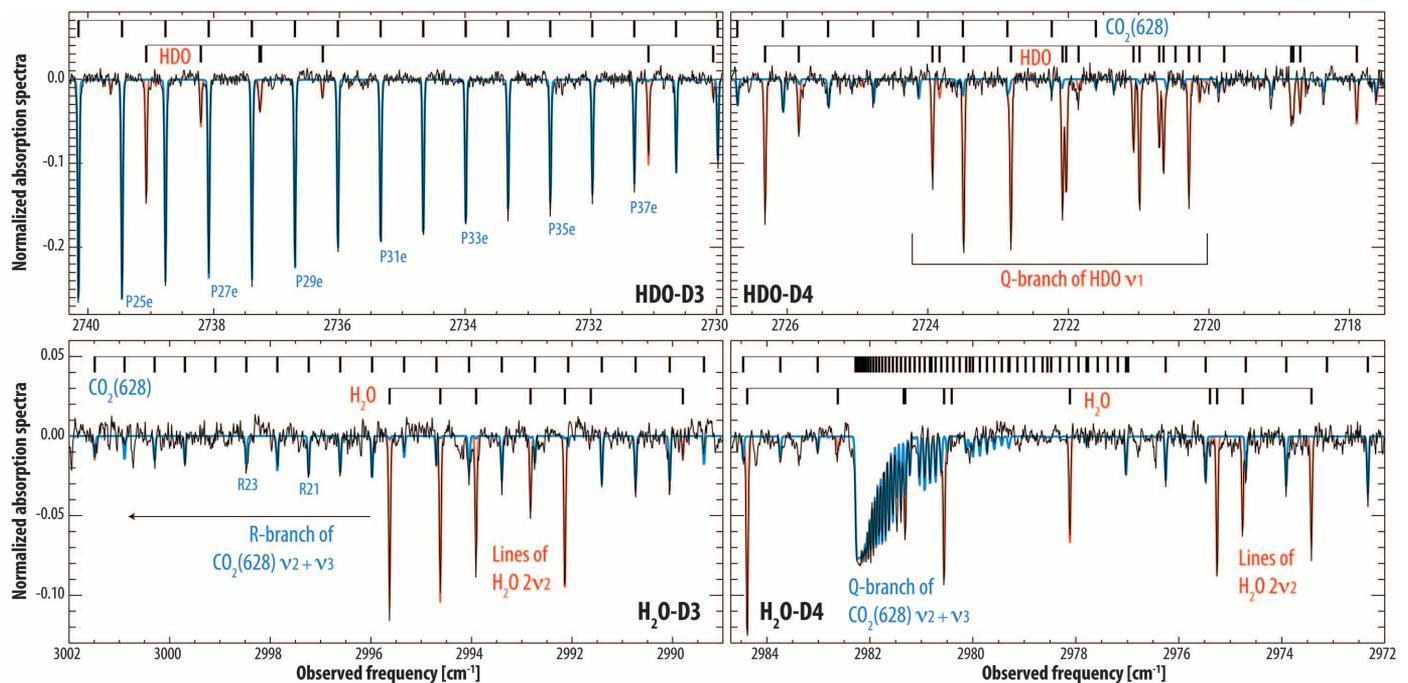
Fig. 1. Mars high-resolution ($\lambda/\delta\lambda$ ~ 100,000) residual spectra of HDO, H_2O, and CO_2 acquired with two settings of CRIRES at VLT on 29 January 2014 (L_s 83°). The data shown were extracted for a field-of-view of 0.2″ (slit width) × 0.256″ (3 pixels along the slit) over Mars's northern hemisphere (latitude, 57° to 69°; longitude, 106° to 133°E). Spectra from detectors D3 and D4 of each CRIRES setting are shown; detectors D1 and D2 reveal additional lines of these species (SM-1). Residual spectral deviation is 0.006 per pixel (1σ). Each martian residual spectrum was derived by subtracting synthetic spectra of the comeasured telluric and solar absorption features (15), after normalizing to the martian continuum. Synthetic models for HDO and H_2O (red trace) and for CO_2 (blue trace) are in good agreement with the measured spectra.
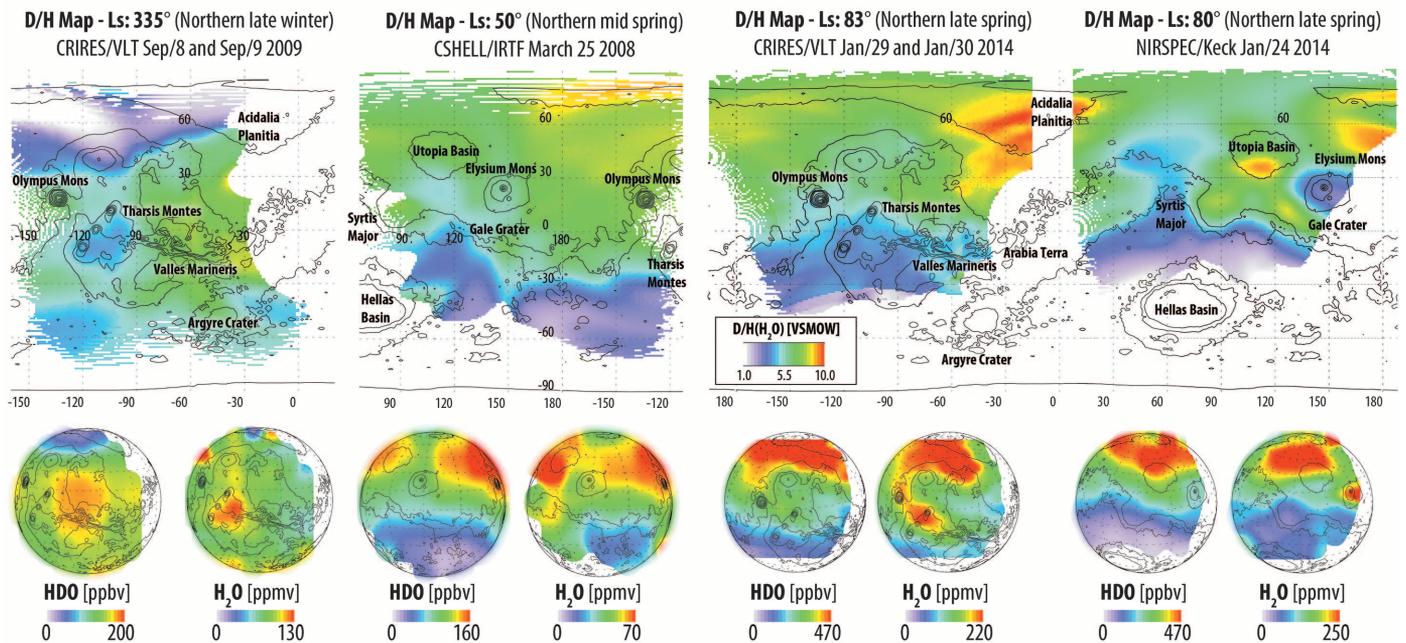
Fig. 2. Maps of HDO and H₂O and their ratio on Mars, obtained at four different seasons (from late northern winter to late northern spring). D/H maps (upper row) were obtained by calculating the ratio of the measured abundance of HDO and H₂O extracted from maps of the individual species (lower row) and are presented relative to the D/H value in Earth's ocean water (VSMOW). The ratio maps (upper row) show the progressive enrichment of D/H in the northern hemisphere as the polar cap sublimes during northern spring. The isotopologue maps (HDO and H₂O) also reveal strong local enhancements and variability but with significant differences between them, associated with global and local climatology. In particular, low D/H values are observed at regions of low temperature and/or high altitude, with high values observed at orographic depressions (e.g., Acidalia Planitia and Utopia Basin).

full disk measurements reflect the mean of diverse regions with low and high D/H, as revealed by our maps (Fig. 2). Moreover, isolated measurements from a discrete region may reflect local climatological effects and so may not represent the deuterium enrichment of the bulk atmosphere. For instance, Gale Crater (location of the MSL Curiosity rover) is at the boundary of a strong gradient between two regions of D/H that range from 1 to 7 VSMOW, where local and seasonal effects may affect retrievals of D/H (L_s 50) (Fig. 2). Our value at Gale Crater (6 VSMOW; L_s 50 and 80) is in good agreement with that derived with the MSL Tunable Laser Spectrometer instrument (6 ± 1 VSMOW) in late 2012 (11). However, our maps reveal that in regions and seasons where both isotopologues are expected to be fully gaseous (equatorial and mid-latitudes during mid and late spring, L_s 50, 83, 80), the atmosphere shows high D/H (~7 VSMOW), with some regions showing strong enrichments reaching 9 to 10 VSMOW.

Temperature is the main parameter governing isotopic ratios in an atmosphere, but other factors such as relative humidity (condensation level), presence of dust particles (condensation nuclei), and dynamical/transport processes (e.g., expansive cooling due to vertical lifting) affect the rate at which condensation occurs for each isotopologue. These factors affect the observable gas phase D/H ratio (see D/H correlations with temperature and water column in SM-3). Models for the seasonal behavior of the D/H ratio on Mars incorporate some of these effects. Using a 3D

general circulation model that included fractionation effects, Montmessin *et al.* (24) predicted hemispheric variability with a peak atmospheric D/H value 15% lower than the value assumed for the polar caps. In general, our results are in agreement with the predicted level of variability with latitude, but the strong local anisotropies observed across the planet will require a more realistic model to account for several climatological processes acting on the isotopologues. Importantly, our typical atmospheric value (7 VSMOW) implies that the permanent polar caps contain a D/H of 8 VSMOW, following the modeling results in (24).

The great obliquity variations experienced by Mars at million-year intervals (27) should have caused all major ice reservoirs to vaporize and reform repeatedly, causing refreshed mixing of water from the different repositories at regular intervals. If so, all near-surface and polar reservoirs of water on Mars should share a relatively common D/H ratio. Because we also observe even higher D/H values (above 8 VSMOW) in certain regions, such mixing would suggest that the current reservoirs of water on Mars contain a higher D/H than initially thought and would consequently require greater loss of water over the planet's lifetime.

Multiple reservoirs have been proposed to account for the current inventory of water on Mars, ranging from the observable PLD (19, 20), to ice-rich regolith at mid-latitudes (28, 29), near-surface reservoirs at high latitudes (30), and subsurface reservoirs as implied by gamma ray and

neutron observations (31). As summarized by Kurokawa *et al.* (32), the PLD can be defined as the minimum estimate of the current inventory of Mars. The PLD would correspond to 1.4 ± 0.3 × 10^18 kg of water [or 10 ± 2 m GEL of water for the north polar region (19)] and 1.6 ± 0.2 × 10^18 kg (11 ± 1.4 m GEL) for the south polar region (20), totaling 21 ± 3.4 m for the PLD reservoir. Recent estimates suggest that the PLD contain 17 to 21 m GEL, with 25 to 29 m GEL across all directly measured reservoirs (33). The initial reservoir of water on Mars (M_p) can be estimated from the current inventory of water on Mars (M_c) and its isotopic ratio (I_c) when knowledge of the ancient isotopic ratio (I_p) exists, together with the fractionation escape rate (f) of the isotopologues, using the relation equation $M_p/M_c = (I_c/I_p)^{[1/(1-f)]}$. From Hubble Space Telescope measurements of D and H Lyman-α emissions in the upper atmosphere of Mars, Krasnopolsky *et al.* (34) derived a fractionation rate of 0.02. Usui *et al.* (35) measured a water D/H of 1.275 VSMOW in melt inclusions (estimated to be 4.5 billion years old) within the Mars meteorite Yamato 980459. Taking this value as I_p and 21 m GEL as M_c, our estimate of 8 VSMOW (for the PLD) as I_c implies that Mars had at least 137 m GEL of water 4.5 billion years ago (see Fig. 3).

This value could be defined as a lower bound for the original GEL because it is based on the minimum current water reservoir (PLD) and neglects the young Sun's high extreme ultraviolet fluxes (36), which would have led to the unfractionated escape of H and D. If we assume
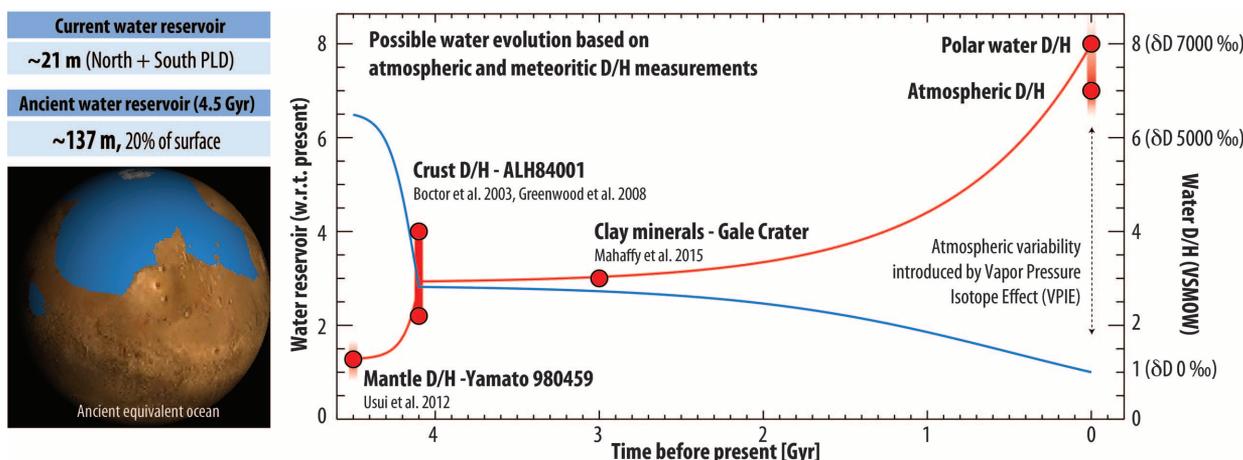
Fig. 3. Isotopic enrichment as evidence for global loss of water on Mars. After correcting for local climatological fractionation of the measured D/H ratio (Fig. 2), the current ratio for D/H in atmospheric water on Mars is at least 7 VSMOW, implying a D/H ratio of 8 VSMOW in the north polar reservoir (red curve and right axis). Assuming a fractionation factor f of 0.02, the D/H ratios obtained from water in Mars meteorites (Yamato 980459, 4.5 billion years old) imply that Mars's initial water reservoir was larger than the current water available on Mars by a factor of at least 6.5 (blue curve and left axis). When considering the current PLD content of 21 m of water, this would imply that at least 137 m GEL of water was present on Mars 4.5 billion years ago, covering 20% of the planet's surface.

that all currently measured water reservoirs (25 to 29 m), including the atmosphere, share the representative 7 VSMOW enrichment, then the ancient estimate is 142 to 165 m, further establishing the 137-m GEL value as a lower bound. Considering Mars's current topography (*37*), 137 m GEL water would have covered up to 20% of the planet's surface (*38*). Meteoritic records dated to 4.1 billion years ago (*39*, *40*) and clay minerals in Gale Crater (*41*) indicate a much higher D/H than in Yamato 980459, implying that the loss of water from Mars occurred in stages (*32*), with a substantial amount of water being lost in the first 0.5 billion years. Geomorphological records on Mars do indicate a wetter past (up to >2000 m GEL), yet—as summarized by Carr and Head (*38*) and more recently confirmed by subsurface observations with the Mars Advanced Radar for Subsurface and Ionosphere Sounding (*42*)—the best estimate is provided by the Vastitas Borealis Formation, which implies 2.3×10^7 km^3 of water (156 m GEL). This estimate is in relatively good agreement with our value (137 m GEL) as inferred from our estimate of D/H enrichment (8 VSMOW) in the PLD. The difference between the two estimates would also mean that ~20 m GEL of water are currently "missing" and could be stored in other proposed water reservoirs (e.g., deep aquifers).

Our D/H maps highlight the importance of obtaining isotopic measurements on Mars that are both spatially and temporally resolved in order to separate climatological from evolutionary effects. Such investigation ultimately leads to a more accurate estimate of the actual D/H of water reservoirs on Mars and improves both the estimate of water loss over geologic time and estimates for the "missing" water that might reside in undiscovered reservoirs. More realistic estimates on current and ancient fractionation rates (e.g., from NASA's Mars Atmosphere and Volatile Evolution Mission) and a larger sample of ancient D/H values derived from authentic (meteorites) and

from drilled and/or returned samples would better constrain the water inventory on Mars, current and past.

REFERENCES AND NOTES

1. M. D. Smith, *Icarus* **167**, 148–165 (2004).
2. M. A. Tschimmel *et al.*, *Icarus* **195**, 557–575 (2008).
3. R. E. Novak, M. J. Mumma, M. A. DiSanti, N. Dello Russo, K. Magee-Sauer, *Icarus* **158**, 14–23 (2002).
4. T. Fouchet *et al.*, *Planet. Space Sci.* **59**, 683–690 (2011).
5. G. L. Villanueva *et al.*, *The Mars Atmosphere: Modeling and Observations Conference*, Williamsburg, VA, 10–13 November 2008, 9101 (Lunar and Planetary Institute, Houston, TX, 2008).
6. M. J. Mumma *et al.*, *Sixth International Conference on Mars*, Pasadena, CA, 20–25 July 2003, 3186 (Lunar and Planetary Institute, Houston, TX, 2003).
7. R. E. Novak, M. J. Mumma, G. L. Villanueva, B. P. Bonev, M. A. Disanti, *Seventh International Conference on Mars*, Pasadena, CA, 9–13 July 2007, 3283 (Lunar and Planetary Institute, Houston, TX, 2007).
8. R. E. Novak, M. J. Mumma, G. L. Villanueva, *Planet. Space Sci.* **59**, 163–168 (2011).
9. G. L. Villanueva *et al.*, *J. Quant. Spectrosc. Radiat. Transf.* **113**, 202–220 (2012).
10. S. Aoki *et al.*, *European Planetary Science Congress 2013*, London, 8–13 September 2013, **8**, EPSC2013-191 (European Planetary Science Congress, Paris, 2013).
11. C. R. Webster *et al.*, *Science* **341**, 260–263 (2013).
12. T. Owen, J. P. Maillard, C. de Bergh, B. L. Lutz, *Science* **240**, 1767 (1988).
13. G. L. Bjoraker, M. J. Mumma, H. P. Larson, *Bull. Am. Astron. Soc.* **21**, 991 (1989).
14. J. P. Grotzinger, *Science* **341**, 1475 (2013).
15. G. L. Villanueva *et al.*, *Icarus* **223**, 11–27 (2013).
16. J.-P. Bibring *et al.*, *Science* **312**, 400–404 (2006).
17. M. H. Carr, *J. Geophys. Res. Planets* **104** (E9), 21897–21910 (1999).
18. W. C. Feldman *et al.*, *J. Geophys. Res. Planets* **109**, E09006 (2004).
19. M. T. Zuber *et al.*, *Science* **282**, 2053–2060 (1998).
20. J. J. Plaut *et al.*, *Science* **316**, 92–95 (2007).
21. M. D. Smith, *J. Geophys. Res. Planets* **107**, 5115 (2002).
22. T. Fouchet *et al.*, *Icarus* **190**, 32–49 (2007).
23. T. Fouchet, E. Lellouch, *Icarus* **144**, 114–123 (2000).
24. F. Montmessin, T. Fouchet, F. Forget, *J. Geophys. Res. Planets* **110**, E03006 (2005).
25. M. C. Malin, B. A. Cantor, M. R. Wu, L. M. Saper, MRO MARCI Weather Reports (2014) (available at www.msss.com/msss_images/subject/weather_reports.html).
26. J. Jouzel, L. Merlivat, *J. Geophys. Res. Atmos.* **89** (D7), 11749 (1984).
27. J. Laskar *et al.*, *Icarus* **170**, 343–364 (2004).
28. J. B. Murray *et al.*, *Nature* **434**, 352–356 (2005).
29. D. P. Page, M. R. Balme, M. M. Grady, *Icarus* **203**, 376–389 (2009).
30. P. H. Smith *et al.*, *Science* **325**, 58–61 (2009).
31. W. V. Boynton *et al.*, *Science* **297**, 81–85 (2002).
32. H. Kurokawa *et al.*, *Earth Planet. Sci. Lett.* **394**, 179–185 (2014).
33. J. Lasue *et al.*, *Space Sci. Rev.* **174**, 155–212 (2013).
34. V. A. Krasnopolsky, M. J. Mumma, G. R. Gladstone, *Science* **280**, 1576–1580 (1998).
35. T. Usui, C. M. O. Alexander, J. Wang, J. I. Simon, J. H. Jones, *43rd Lunar and Planetary Science Conference*, The Woodlands, TX, 19–23 March 2012, 1341 (Lunar and Planetary Institute, Houston, TX, 2012).
36. W. Lammer, *Springer Briefs in Astronomy* **174**, 113–154 (2012).
37. D. E. Smith *et al.*, *J. Geophys. Res. Planets* **106** (E10), 23689 (2001).
38. M. H. Carr, J. W. Head, *J. Geophys. Res. Planets* **108**, 5042 (2003).
39. N. Z. Boctor, C. M. O. D. Alexander, J. Wang, E. Hauri, *Geochim. Cosmochim. Acta* **67**, 3971–3989 (2003).
40. J. P. Greenwood, S. Itoh, N. Sakamoto, E. P. Vicenzi, H. Yurimoto, *Geophys. Res. Lett.* **35**, L05203 (2008).
41. P. R. Mahaffy *et al.*, *Science* **347**, 412–414 (2015).
42. J. Mouginot, A. Pommerol, P. Beck, W. Kofman, S. M. Clifford, *Geophys. Res. Lett.* **39**, L02202 (2012).

Editor's Summary

Mapping Mars' water history

We know the water cycle on Earth is complex. Neither is it simple on Mars. Infrared maps of water isotopes made by Villanueva *et al.* show the distribution of H_2O and "semiheavy" water (HDO: deuterated water containing a mixture of hydrogen isotopes) across Mars. HDO enrichment varies with time and location; for example, irregular isotopic signals associate with different terrain features. The measurements also allow seasonal sublimation levels of the northern ice cap to be estimated and thus could be used to reveal past climate behavior.

Science, this issue p. 218

Article Tools	Visit the online version of this article to access the personalization and article tools: http://science.sciencemag.org/content/348/6231/218
Permissions	Obtain information about reproducing this article: http://www.sciencemag.org/about/permissions.dtl